Journal of Radioanalytical and Nuclear Chemistry (2019) 320:561–568
https://doi.org/10.1007/s10967-019-06510-z

^{93}Nb(n,2n)^{92m}Nb, ^{93}Nb(n,α)^{90m}Y and ^{92}Mo(n,p)^{92m}Nb reactions at 14.78 MeV and covariance analysis

Imran Pasha[1] · Rudraswamy Basavanna[1] · Santhi Sheela Yerranguntla[2] · Saraswatula Venkata Suryanarayana[3] · Meghna Karkera[2] · Haladhara Naik[4] · Manjunatha Prasad Karantha[2,5] · Laxman Singh Danu[3] · Saroj Bishnoi[6] · Tarun Patel[6] · Rajeev Kumar[7]

Received: 4 December 2018 / Published online: 9 April 2019

Abstract
The cross sections for the ^{93}Nb(n,2n)^{92m}Nb, ^{93}Nb(n,α)^{90m}Y and the ^{92}Mo(n,p)^{92m}Nb reactions have been measured with respect to the ^{197}Au(n,2n)^{196}Au monitor reaction at the incident neutron energy of 14.78 ± 0.19 MeV by employing methods of activation and off-line γ-ray spectrometry. The covariance analysis was carried out by taking into consideration of partial uncertainties in different attributes and correlation among the attributes. The present data have been compared with the literature data available in EXFOR, evaluated data of different libraries and theoretical values based on TALYS-1.8 code.

Keywords ^{93}Nb(n,2n)^{92m}Nb, ^{93}Nb(n,α)^{90m}Y and ^{92}Mo(n,p)^{92m}Nb reactions · Cross sections · ^{3}H(d,n)^{4}He reaction neutron · Activation and off line γ-ray spectrometry · Covariance analysis · TALYS-1.8

Introduction

The neutron induced reaction cross sections are very useful in various field such as in the nuclear technology, for the investigation of nuclear theory, to explain the nuclear reaction mechanism and in fusion reactor facility [1–4]. The cross section of ^{93}Nb(n,2n)^{92m}Nb reaction is used as a flux monitor for the 14 MeV neutron generator [5–7]. The natural niobium metal has high-melting point and thus is used as an element of superconductor alloys in fusion reactors, as a structural material in thermonuclear reactors and for the advance reactor design [8–10]. Niobium also finds very important applications in nuclear reactors as a cladding, structural, corrosion barrier material due to its good physical, chemical properties and low neutron absorption cross section [11–15]. On the other hand molybdenum is used as a structural material in the nuclear fission and future fusion reactors, alloying element in different advanced nuclear energy systems, as an important constituent in the first wall of a fusion reactor, and has potential applications in neutronics [16–23].

Different types of reaction cross sections data of niobium and molybdenum at higher neutron energies plays important role in the construction of different types of nuclear reactors [24–26]. This is because in reactor, the neutron energy ranges from eV to 20 MeV [27]. The evaluation of excitation function of ^{93}Nb(n,2n)^{92m}Nb reaction in the energy range from threshold to 40 MeV was carried out by the means of the statistical analysis of experimental cross section data and data from theoretical model calculations, the readers are refer work carried out by Zolotarev [28]. The evaluation of excitation function of ^{92}Mo(n,p)^{92m}Nb reaction in the energy range from 1 to 40 MeV was carried out by the means of the generalized least square method within the PADE-2 code,

✉ Haladhara Naik
naikhbarc@yahoo.com

1 Department of Physics, Bangalore University, Bengaluru, Karnataka 560056, India

2 Department of Statistics, Manipal Academy of Higher Education, Manipal, Karnataka 576104, India

3 Nuclear Physics Division, Bhabha Atomic Research Center, Mumbai 400085, India

4 Radio Chemistry Division, Bhabha Atomic Research Center, Mumbai 400085, India

5 Center for Advanced Research in Applied Mathematics and Statistics, Manipal Academy of Higher Education, Manipal, Karnataka 576104, India

6 Neutron and X-ray Physics Division, Bhabha Atomic Research Center, Mumbai 400085, India

7 Reactor Physics Design Division, Bhabha Atomic Research Center, Mumbai 400085, India

the readers are refer work carried out by Zolotarev et al. [29].

In view of the above facts, it is important to study the (n,2n), (n,α), (n,p) cross section of ^{93}Nb and ^{92}Mo at the higher neutron energy range of 14–20 MeV. On the basis of literature survey, few experimental cross sections data for the ^{93}Nb(n,2n)^{92m}Nb [30–32], ^{93}Nb(n,α)^{90m}Y [22] and ^{92}Mo(n,p)^{92m}Nb reactions are available in EXFOR compilation [33] at the neutron energy of 14.78 ± 0.19 MeV. Considering the importance of cross section data at higher neutron energy, we have measured the cross section of ^{93}Nb(n,2n)^{92m}Nb, ^{93}Nb(n,α)^{90m}Y and ^{92}Mo(n,p)^{92m}Nb reactions at the neutron energy of 14.78 ± 0.19 MeV by employing methods of activation and off-line γ-ray spectrometry.

We have followed the relative technique for estimating the cross section of ^{93}Nb(n,2n)^{92m}Nb, ^{93}Nb(n,α)^{90m}Y and ^{92}Mo(n,p)^{92m}Nb reactions for which the ^{197}Au(n,2n)^{196}Au reaction was considered as a monitor to estimate the neutron flux. The uncertainty propagation of the measured reaction cross sections data was carried out by taking into account partial uncertainties in different attributes and the correlation among those using method of covariance. The cross sections of ^{93}Nb(n,2n)^{92m}Nb, ^{93}Nb(n,α)^{90m}Y and ^{92}Mo(n,p)^{92m}Nb reactions as a function of neutron energy within the range of 12–18 MeV were theoretically calculated by using TALYS-1.8 code [34] with default parameters and are compare with the present experimental data.

Experimental details

The measurement was carried out by making use of the neutron generator constructed based on the Cockcroft–Walton voltage multiplier accelerator of Purnima at Bhabha atomic research center (BARC), Mumbai. In Purnima neutron generator the D^+ ions were accelerated up to 300 kV. The D^+ ions are generated in an RF ion source, which is extracted, focused, accelerated and incident on a tritium target. The deuteron ions incident on titanium–tritium (TiT) target was maintain at ground potential to produce 14.1 MeV neutrons through the ^{3}H(d,n)^{4}He reaction [35]. In the present measurement the D^+ ion is accelerated to 99.71 kV which was impinge on titanium–tritium (TiT) target. This collision produces neutrons of energy 14.78 ± 0.19 MeV in the laboratory frame through the ^{3}H(d,n)^{4}He (Q = 17.59 MeV) reaction, at nearly forward angles. The neutron energy is nearly constant at forward angles up to ± 10° in laboratory frame, as shown in Fig. 9 of Ref. [36]. In our experimental set up, the sample area is about 1 cm^2 and is at a distance of 1.5 cm from the neutron generating target. The area of target covers an angle of 1 cm/(2 * pi * 1.5 cm) * (180°) ~ 19.1°. Considering that target has maximum angular coverage of about 10°, the half angle is ± 5° on either side of beam. Therefore, neutron energy variation over 5°–10° is negligible.

The weights of ^{93}Nb, ^{nat}Mo and ^{197}Au metal foils are 198.8, 165.8 and 334.3 mg, respectively. They were wrapped with 0.011 mm thick Al foil to shield the radioactive contamination from one another during the neutron irradiation. A stack of Au–Nb–Mo samples was mounted at zero degree angle relative to the beam direction. The stack foils of Au–Nb–Mo was irradiated for 1.5 h with the neutron beam produced from the ^{3}H(d,n)^{4}He reaction. After the irradiation, samples were taken out and cooled for 0.3–1.2 h. A diagrammatic arrangement of the Au–Nb–Mo stack is illustrated in Fig. 1. The radioactive samples of Nb, Mo and Au along with Al wrapper were mounted on different Perspex plates and then taken for γ-ray spectrometry. The γ-ray counting of the irradiated Nb, Mo and Au foils were carried out using a lead shielded pre-calibrated 185-cc Baltic HPGe detector having 30% relative efficiency and coupled to a PC-based 4096 channel analyzer. The γ-ray counting dead time was always kept less than 5% by keeping the mounted samples of Nb, Mo and Au foils at a suitable distance from the detector end cap. The data acquisition was done using a CAMAC based LAMPS (Linux Advance Multi Parameter System) software. The energy and efficiency calibrations of the HPGe detector were carried out by counting the characteristic γ-ray energies of ^{152}Eu standard source, at the same geometry to reduce coincidence summing effect. The resolution of the HPGe detector has a FWHM of 1.8 keV at 1.33 MeV γ-ray for ^{60}Co. The γ-ray activity of ^{196}Au produced from the ^{197}Au(n,2n) monitor reaction was used to measure the neutron flux.

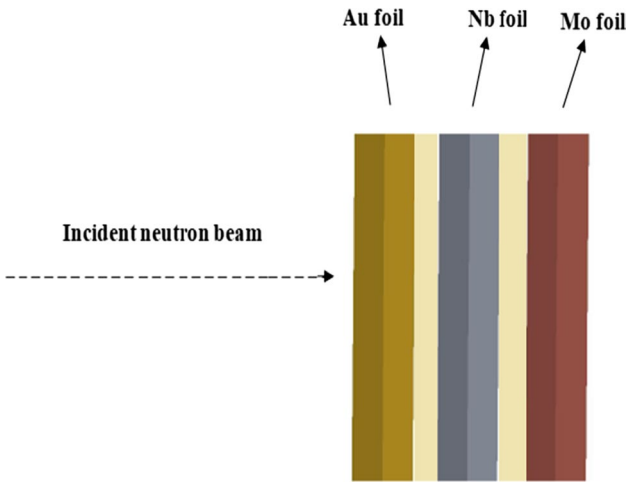

Fig. 1 Schematic arrangement of stack of Au–Nb–Mo foils

Data analysis and results

Estimation of efficiency calibration with covariance analysis

The efficiency $\varepsilon(E_\gamma)$ calibration of the HPGe detector system was done by using a ^{152}Eu point source from their known characteristic γ-ray energies. The efficiency of HPGe detector system was estimated by using following relation.

$$\varepsilon(E_\gamma) = \frac{CK_C}{I_\gamma A_0 e^{-0.693t/T_{1/2}}} \quad (1)$$

where E_γ is γ-ray energy, C is counts for 3600 s, which was obtained from the measured ^{152}Eu γ-ray spectrum, source activity $A_0 = 6659.21 \pm 81.60$ Bq as on 1 October 1999, $T_{1/2}$ is the half-life (13.517 ± 0.014 y) of ^{152}Eu, t is elapsed time between source and detector calibration (18.53 y). The γ-ray abundance, I_γ for the γ-ray energies of interest were retrieved from NuDat 2.7 database [37, 38]. The correction factor due to coincidence summing effect K_C was estimated using Monte Carlo simulation code EFFTRAN [39], by making use of structural data of HPGe detector such as dimension, crystal hole cavity, crystal material, end cap, mount cup, absorber, window and calibration source description. There is small statistical uncertainty in coincidence summing corrections factors, which does not exceed 1%. The known data of attributes are substituted in Eq. (1) to obtained efficiency $\varepsilon(E_\gamma)$ at each of the specified γ-ray energy of ^{152}Eu source and the same are presented in column 5 of Table 1.

From Eq. (1) we have identified four attributes C, I_γ, A_o and λ that contributes to the uncertainty in efficiency. The partial uncertainties due to each of the attributes mentioned above and their correlations for constructing the covariance matrix V_ε are obtained by following the methodology as given in refs. [40, 41].

The characteristic γ-ray energies of the ^{92m}Nb, ^{90m}Y, ^{92m}Nb and ^{196}Au in the irradiated foils are different from the known γ-ray energies of ^{152}Eu source. Hence to estimate the efficiencies corresponding to the characteristic γ-rays of ^{92m}Nb, ^{90m}Y, ^{92m}Nb and ^{196}Au reaction products, we have chosen an empirical relation as a model through interpolation using the following linear parametric function

$$Z = \ln(\varepsilon_i) = \sum_{k=1}^{m} p_k (\ln[E_i])^{k-1} \quad 1 \le i \le 8,\ 1 \le k \le m \quad (2)$$

In the present calculations, the best fit was achieved for $n = 4$, with $\frac{\chi^2}{8-4} = 1.36 \approx 1$. We consider the following linear parametric model as the best model, which is presented below.

$$\ln \varepsilon = -3.941 - 0.879 \ln E + 0.397(\ln E)^2 + 0.191(\ln E)^3 \quad (3)$$

We use Eq. (3) and estimate efficiency at energies corresponding to characteristic γ-rays emitted from the ^{92m}Nb, ^{90m}Y, ^{92m}Nb and ^{196}Au nuclides. The interpolated efficiencies along with the measured values of efficiency are shown in Fig. 2. The efficiencies at these γ-ray energies along with covariance information are required for further calculations. We follow the same methodology for generation of covariance matrix as given in refs. [40–42]. The results of interpolated detector efficiencies along with covariance and correlation matrix are presented in Table 2.

Table 1 Efficiency of HPGe detector based on standard ^{152}Eu source

E_γ (keV)	I_γ (%)	C	K_c	$\varepsilon(E_\gamma)$
121.8	28.53 ± 0.16	258,872 ± 3570	1.236	1.208E−01
244.7	7.55 ± 0.04	45,274 ± 440	1.351	8.720E−02
344.3	26.59 ± 0.20	131,156 ± 678	1.151	6.116E−02
411.1	2.237 ± 0.013	7828 ± 229	1.405	5.296E−02
488.6	0.414 ± 0.003	1211 ± 112	1.447	4.559E−02
688.6	0.856 ± 0.006	2065 ± 58	1.088	2.828E−02
867.3	4.23 ± 0.03	6178 ± 90	1.424	2.240E−02
1008.6	10.11 ± 0.05	18,762 ± 302	0.901	1.801E−02

Estimation of ^{93}Nb(n,2n)^{92m}Nb, ^{93}Nb(n,α)^{90m}Y and ^{92}Mo(n,p)^{92m}Nb reaction cross sections with covariance analysis

The cross section of ^{93}Nb(n,2n)^{92m}Nb, ^{93}Nb(n,α)^{90m}Y and ^{92}Mo(n,p)^{92m}Nb reactions at the neutron energy of 14.78 ± 0.19 MeV were determined by ratio method using the following relation,

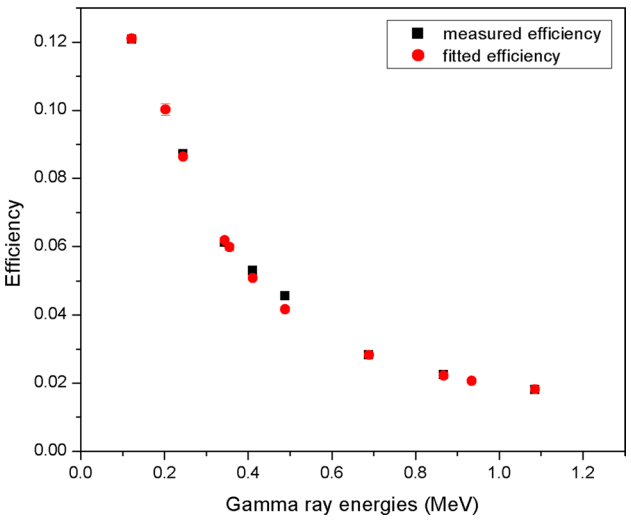

Fig. 2 Comparison between measured and fitted efficiencies

Table 2 Interpolated efficiencies of the detector and correlation matrix

Nuclide	γ-ray energy (keV)	ε_c	$V_{\varepsilon c}$ ($\times 10^{-07}$)				$C_{\varepsilon c}$			
^{92m}Nb	934.4	0.0206 ± 0.0003	1.197				1			
^{90m}Y	202.5	0.1002 ± 0.0017	2.291	29.32			0.39	1		
^{92m}Nb	934.4	0.0206 ± 0.0003	1.197	2.292	1.197		1	0.39	1	
^{196}Au	355.7	0.0598 ± 0.0009	2.144	9.003	2.144	7.656	0.71	0.60	0.71	1

$$\sigma_s = \sigma_M \frac{C_S \lambda_S W t_M a_M A_{VS} I_{\gamma M} \varepsilon(E_\gamma)_M \left(1 - e^{-\lambda t_{iM}}\right)\left(e^{-\lambda t_{dM}}\right)\left(1 - e^{-\lambda t_{cM}}\right)}{C_M \lambda_M W t_S a_S A_{VM} I_{\gamma S} \varepsilon(E_\gamma)_S \left(1 - e^{-\lambda t_{iS}}\right)\left(e^{-\lambda t_{dS}}\right)\left(1 - e^{-\lambda t_{cS}}\right)} \prod_k \frac{(C_k)_m}{(C_k)_S} \tag{4}$$

where S and M in subscript denotes the sample and monitor, $\sigma_s(E_n)$ and $\sigma_M(E_n)$ are reaction cross section at the neutron energy E_n respectively, C_S and C_M are the observed γ-ray peak counts of the reaction products ^{92m}Nb, ^{90m}Y, ^{92m}Nb and ^{196}Au, respectively, λ_S and λ_M are decay constants, Wt_S and Wt_M are weights, a_S and a_M are isotopic abundances, A_{VS} and A_{VM} are average atomic masses, $I_{\gamma S}$ and $I_{\gamma M}$ are the γ-ray abundances, $\varepsilon(E_\gamma)_S$ and $\varepsilon(E_\gamma)_M$ are efficiencies of detector relative to characteristics γ-rays of radionuclide, t_i, t_d and t_C denote irradiation, cooling and counting time, $(C_k)_S$ and $(C_k)_m$ are the correction factors for the kth attribute, where k indicates the dead time of HPGe detector $\left(\frac{\text{clock time}}{\text{live time}}\right)$ and γ-ray self-attenuation factor (Γ_{attn}). The self-attenuation factor (Γ_{attn}) for the activation foils were estimated by using the relation [43] $\Gamma_{attn} = \frac{1-e^{-\mu l}}{\mu l}$, where l is the thickness of the each foil and μ is mass attenuation coefficient retrieved from XMuDat ver. 1.0.1 [44]. The monitor cross section of ^{197}Au(n,2n)^{196}Au reaction at the neuron energy 14.78 ± 0.19 MeV was obtained by linear interpolation method by considering the cross section values at the nearest energy points, which is obtained as 2.160 ± 0.0198 barns (IRDF 1.05, [45]).

The essential data of the attributes, which are half-life, isotopic abundances, γ-ray abundances with uncertainties are presented in Table 3 and average atomic mass with uncertainties data's are retrieved from NuDat 2.7 database [37]. The attributes observed with error are σ_M, C_S, C_M, λ_S, λ_M, Wt_S, Wt_M,a_S, A_{VS},A_{VM}, $I_{\gamma S}$, $I_{\gamma M}$,$\varepsilon(E_\gamma)_S$, $\varepsilon(E_\gamma)_M$, $(\Gamma_{attn})_S$, $(\Gamma_{attn})_M$ and other attributes a_M,t_i, t_d, t_C are observed without error.

The covariance matrix $V_{\sigma S}$ [46] corresponding to the experimentally measured reaction cross sections is given by

$$(V_{\sigma S})_{ij} = \sum_{kl} (e_k)_i (s_{kl})_{ij} (e_l)_j, \quad 1 \le i, j \le 3, \ 1 \le k, \ l \le 16 \tag{5}$$

where $(s_{kl})_{ij}$ is the micro-correlation between ith, jth observations due kth, lth attributes, respectively and $(e_k)_i = \frac{\partial \sigma_{Si}}{\partial (x_k)_i} \Delta(x_k)_i$, $(e_l)_j = \frac{\partial \sigma_{Sj}}{\partial (x_l)_j} \Delta(x_l)_j$ is partial uncertainties in σ_{Si}, σ_{Sj} due to the kth, lth attributes, respectively. The partial uncertainties from different attributes present in the measured reactions of ^{93}Nb(n,2n)^{92m}Nb, ^{93}Nb(n,α)^{90m}Y and ^{92}Mo(n,p)^{92m}Nb cross section with respect to ^{197}Au(n,2n)^{196}Au monitor reaction are listed in Table 4. The correlations obtained between three observations are listed in the last column of Table 4. Detailed descriptions on micro correlation matrices, the readers are refer work carried out by Santhi Sheela et al. [47]. The results of the measured reactions ^{93}Nb(n,2n)^{92m}Nb, ^{93}Nb(n,α)^{90m}Y and ^{92}Mo(n,p)^{92m}Nb cross section at the neutron energy of 14.78 ± 0.19 MeV with its uncertainties and correlations matrix are presented in Table 5.

Table 3 Isotopic abundance and basic nuclear spectroscopic data of reaction product required for the estimation of $\sigma_s(E_n)$

Nuclear reaction	Threshold energy (MeV)	Isotopic abundance of target (%)	Product nuclide	Half-life	γ-ray energy (keV)	γ-ray abundance (%)	Mode of decay (%)
^{93}Nb(n,2n)	8.927	100	^{92m}Nb	10.15 ± 0.02 d	934.4	99.15 ± 0.04	EC (100)
^{93}Nb(n,α)	0.0	100	^{90m}Y	3.19 ± 0.06 h	202.5	97.3 ± 0.4	IT(99.99) + β$^-$(0.0018)
^{92}Mo(n,p)	0.0	14.53 ± 0.03	^{92m}Nb	10.15 ± 0.02 d	934.4	99.15 ± 0.04	EC (100)
^{197}Au(n,2n)	8.114	100	^{196}Au	6.1669 ± 0.0006 d	355.7	87 ± 3	EC(93) + β^-(7)

Table 4 Detailed of partial uncertainties and correlations from the different attributes of measured reactions relative to monitor reaction

Attributes	Nuclide ^{92m}Nb	Nuclide ^{90m}Y	Nuclide ^{92m}Nb	Correlation
Monitor reaction cross section σ_M	4.682E−03	4.768E−05	5.743E−04	Correlated
γ-ray peak counts C_S	2.742E−02	1.842E−04	9.289E−03	Uncorrelated
γ-ray peak counts C_M	2.861E−03	2.913E−05	3.509E−04	Fully correlated
Decay constant λ_S	2.887E−05[a]	4.168E−06[b]	2.287E−06[c]	a and c are fully correlated c is uncorrelated
Decay constant λ_M	4.436E−06	4.518E−08	5.441E−07	Fully correlated
Weight of sample Wt_S	1.777E−04[a]	1.809E−06[b]	1.818E−05[c]	a and b are fully correlated c is uncorrelated
Weight of monitor Wt_M	8.813E−05	8.975E−07	1.081E−05	Fully correlated
Isotopic abundance a_S	–[a]	–[b]	1.292E−04[c]	a and b found to be with no error and c with error
Average atomic mass A_{VS}	8.788E−09[a]	8.949E−11[b]	1.158E−10[c]	a and b are fully correlated c is uncorrelated
Average atomic mass A_{VM}	1.554E−09	1.583E−11	1.907E−10	Fully correlated
γ-rayabundance $I_{\gamma S}$	2.059E−04[a]	2.136E−06[b]	2.525E−05[c]	a and c are fully correlated b is uncorrelated
γ-rayabundance $I_{\gamma M}$	1.759E−03	1.792E−05	2.159E−04	Fully correlated
Efficiency of detector $\varepsilon(E_\gamma)_S$	8.540E−03[a]	8.875E−05[b]	1.047E−03[c]	a and c are fully correlated b is uncorrelated
Efficiency of detector $\varepsilon(E_\gamma)_M$	7.463E−03	7.601E−05	9.154E−04	Fully correlated
γ-attenuation coefficient $(\Gamma_{attn})_S$	7.515E−04	2.894E−05	8.959E−05	Uncorrelated
γ-attenuation coefficient $(\Gamma_{attn})_M$	8.812E−05	8.944E−07	1.081E−05	Fully correlated

Table 5 The experimentally estimated reaction cross sections relative to the ^{197}Au(n,2n)^{196}Au monitor reaction with its uncertainty and correlation matrix

Reaction	Cross section (barns)	Correlation matrix		
^{93}Nb(n,2n)^{92m}Nb	0.5103 ± 0.03365	1		
^{93}Nb(n,α)^{90m}Y	0.0052 ± 0.00027	0.28	1	
^{92}Mo(n,p)^{92m}Nb	0.0626 ± 0.00968	0.14	0.12	1

Discussion

The cross sections for the ^{93}Nb(n,2n)^{92m}Nb, ^{93}Nb(n,α)^{90m}Y and the ^{92}Mo(n,p)^{92m}Nb reactions have been measured with respect to ^{197}Au(n,2n)^{196}Au monitor reaction at the neutron energy of 14.78 ± 0.19 MeV by employing methods of activation and off-line γ-ray spectrometry. The efficiency of HPGe detector was carried out using standard ^{152}Eu source and the cross sections of three different reactions were determined using ratio method. We estimated uncertainties considering various attributes in the data using the covariance analysis and correlations between them. The computer code TALYS-1.8 [34] was used for the analysis and prediction of nuclear reaction cross sections values based on the nuclear models. In the present work, the cross sections for the ^{93}Nb(n,2n)^{92m}Nb and ^{93}Nb(n,α)^{90m}Y reactions within the neutron energy range of 12–18 MeV were theoretically calculated using the TALYS-1.8 code with default parameters. The present experimental data of ^{93}Nb(n,2n)^{92m}Nb reaction at the neutron energy of 14.78 ± 0.19 MeV, the evaluated data from JEFF-3.3 [48], ROSFOND [49], IRDFF-1.02 [50], JENDL/AD [51] and EAF [52] libraries, literature data [2–4, 6, 8–15, 30] from EXFOR [33], as well as the theoretically calculated values from TALYS-1.8 code [34] within 12–18 MeV are shown in Fig. 3. It is observed from Fig. 3, that the ^{93}Nb(n,2n)^{92m}Nb reaction cross section of present measurement at the neutron energy of 14.78 ± 0.19 MeV is in excellent agreement with the theoretical value from TALYS-1.8 and in close agreement with the evaluated data from JEFF-3.3, ROSFOND, IRDFF-1.02 and JENDL/AD, EAF libraries as well as with the literature data present in EXFOR [33].

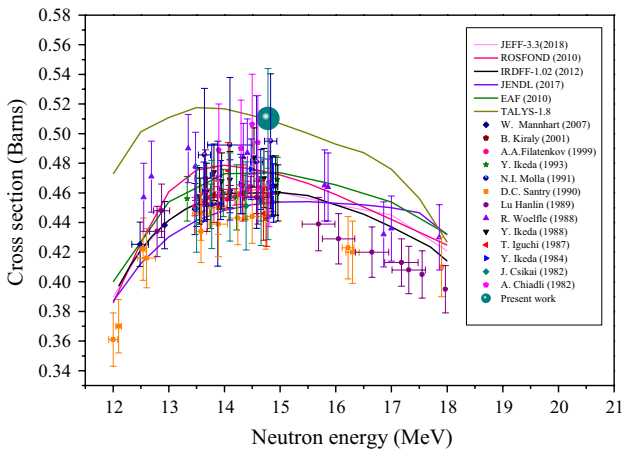

Fig. 3 Comparison of ^{93}Nb(n,2n)^{92m}Nb reaction cross section from the present work with the literature data, evaluated data of JEFF-3.3, ROSFOND, IRDF-1.02, JENDL/AD and EAF libraries as well as with the theoretical value from TALYS-1.8 within the neutron energy range of 12–18 MeV

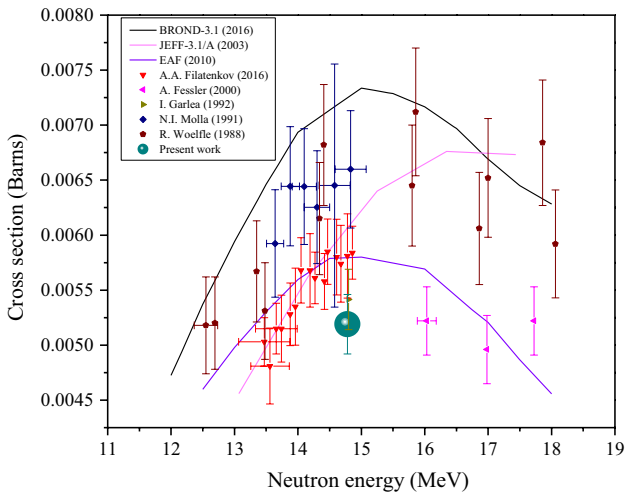

Fig. 4 Comparison of ^{93}Nb(n,α)^{90m}Y reaction cross section from the present work with the literature data, evaluated data of BROND-3.1, JEFF-3.1/A and EAF libraries within the neutron energy range of 12–18 MeV

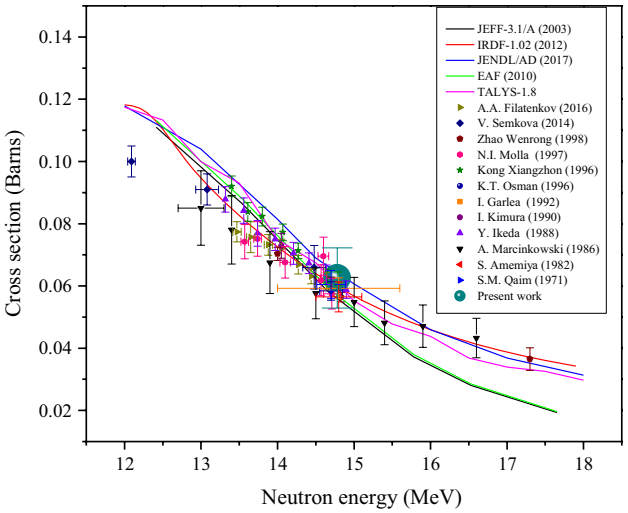

Fig. 5 Comparison of ^{92}Mo(n,p)^{92m}Nb reaction cross section from the present work with the literature data, evaluated data of JEFF-3.1/A, IRDF-1.02, JEND and/AD, EAF libraries as well as with the theoretical value of TALYS-1.8 within the neutron energy of 12–18 MeV

The experimentally measured cross section of ^{93}Nb(n,α)^{90m}Y reaction at the neutron energy of 14.78 ± 0.19 MeV, the evaluated data from BROND-3.1 [53], JEFF-3.1/A [54], EAF [52] libraries and literature data [8, 11, 24, 25, 32] from EXFOR [33], within the neutron energy range of 12–18 MeV are shown in Fig. 4. It is observed from Fig. 4 that the cross section of ^{93}Nb(n,α)^{90m}Y reaction from present work at the neutron energy of 14.78 ± 0.19 MeV is in close agreement with the literature data [8, 11, 24, 25, 32], evaluated data of JEFF-3.1/A and EAF libraries but not with that of BROND-3.1 library.

The experimentally measured cross section of ^{92}Mo(n,p)^{92m}Nb reaction at the neutron energy of 14.78 ± 0.19 MeV, the evaluated data from JEFF-3.1/A [54], IRDFF-1.02 [50], JENDL/AD [51] and EAF [52] libraries, literature data [12, 17–23, 25–27, 32] from EXFOR [33], as well as the theoretical values from TALYS-1.8 code [34] within the neutron energy range of 12–18 MeV are shown in Fig. 5. It is observed from Fig. 5 that the cross section of ^{92}Mo(n,p)^{92m}Nb reaction from the present work at the neutron energy of 14.78 ± 0.19 MeV is in excellent agreement with the evaluated data from JEFF-3.1/A, IRDFF-1.02, JENDL/AD, and EAF libraries as well as with the theoretical values from TALYS-1.8.

Conclusion

The cross section for the ^{93}Nb(n,2n)^{92m}Nb, ^{93}Nb(n,α)^{90m}Y and the ^{92}Mo(n,p)^{92m}Nb reactions have been measured relative to the ^{197}Au(n,2n)^{196}Au monitor reaction at the neutron energy of 14.78 ± 0.19 MeV by using the methods of activation and off-line γ-ray spectrometry. The efficiency of HPGe detector was calculated by using ^{152}Eu standard source along with coincidence summing effect (K_C). The interpolation method is chosen based on minimum Chi square test to estimate the efficiency of unknown γ-ray energies. The uncertainties in all attributes for the cross sections was taken carefully and performed using error analysis, micro-correlation of all attributes. We executed covariance analysis method to estimate uncertainties of the cross sections data, which was carried out using error analysis and micro-correlation. The cross sections of ^{93}Nb(n,2n)^{92m}Nb, ^{93}Nb(n,α)^{90m}Y and ^{92}Mo(n,p)^{92m}Nb reactions from the present studies have been compared and found to be in close agreement with the evaluated data of various libraries, literature data available in EXFOR and theoretically calculated values based on TALYS-1.8.

Acknowledgements The research was financially assisted by Department of atomic energy & Board of research in nuclear sciences (DAE-BRNS) through major research project (Sanction No. 36(6)/14/92/2014-BRNS/2727) and Directorate of Minority, Govt. of Karnataka. We would like to thank the employees of Purnima neutron generator for their kind support to carryout neutron irradiation experiment. The authors would like to thank S. Ganesan, HBNI, BARC, Mumbai for the valuable suggestions and Tim Vidmar, Belgian Nuclear Research Center (SCK CEN), Belgium for supplied the EFFTRAN software.

References

1. Wenrong Z, Hanlin L, Weixiang Y, Xialin Y (1989) Compilation of measurement and evaluations of nuclear activation cross section for nuclear data applications. INDC (CPR)-16

2. Mannhart W, Schmidt D (2007) Measurement of neutron activation cross sections in the energy range from 8 MeV to 15 MeV. Report of the Physikalisch-Technischen Bundesanstalt, Braunschweig
3. Kiraly B, Csikai J, Doczi R (2001) Validation of neutron data libraries by differential and integral cross sections. JAERI 6:283–288
4. Filatenkov AA, Chuvaev SV, Aksenov VN, Yakovlev VA, Malyshenkov AV, Vasil'ev SK, Avrigeanu M, Avrigeanu V, Smith DL, Ikeda Y, Wallner A, Kutschera W, Priller A, Steier P, Vonach H, Mertens G, Rochow W (1999) Systematic measurement of activation cross sections at neutron energies from 13.1 to 14.9 MeV. Report Khlopin Radiev Inst, Leningrad Reports, Russia
5. Ichihara A (2016) Calculation of cross section for meta-stable state production in the (n, γ), (n, n'), (n,2n) and (n,3n) reactions of 93Nb. J Nucl Sci Technol 53:2049–2055
6. Ikeda Y, Konno C, Oyama Y, Kosako K, Oishi K, Maekawa H (1993) Absolute measurement of activation cross sections of 27Al(n, p)27Mg, 27Al(n, a)24Na, 56Fe(n, p)56Mn,90Zr(n,2n)89m+gZr and 93Nb(n,2n)92mNb at energy range of 13.3–14.9 MeV. J Nucl Sci Technol 30(9):870–880
7. Goldberg DC, Dicker G, Worcester SA (1972) Niobium and niobium alloys in nuclear power. Nucl Eng Des 22:95–123
8. Molla NI, Miah RU, Rahman M, Akhter A (1991) Excitation functions of some (n, p), (n,2n) and(n, α) reactions on nickel, zirconium and niobium isotopes in the energy range 13.63–14.83 MeV. Nucl Data Sci Technol Juelich 91:355
9. Santry DC, Werner RD (1990) Cross sections for the ^{93}Nb(n,2n)^{92m}Nb reaction. Can J Phys 68:582
10. Hanlin L, Wenrong Z, Weixiang Y, Xiaogang H (1989) Neutron activation cross section measurements and evaluations in CIAE. INDC(CPR)-16
11. Wolfle R, Mannan A, Qaim SM, Liskien H, Widera R (1988) Excitation functions of 93Nb(n,2n)92mNb, 93Nb(n, α)90 m, gY, 139La(n, α)136Cs and 181Ta(n, p)181Hf reactions in the energy range of 12.5–19.6 MeV. Appl Radiat Isotopes 39:407–412
12. Ikeda Y, Konno C, Oishi K, Nakamura T, Miyade H, Kawade K, Yamamoto H, Katoh T (1988) Activation cross section measurement for fusion reactor structural materials at neutron energy from 13.3 to 15.0 MeV using FNS facility. Report JAERI 1312
13. Iguchi T, Nakata K, Nakazawa M (1987) Improvement of accuracy of Zr/Nb activation-rate ratio method for D-T neutron source determination. J Nucl Sci Technol 24(12):1076–1079
14. Ikeda Y, Miyade H, Kawade K, Yamamoto H (1984) Measurement of high threshold reaction cross sections for 13.5 to 15 MeV. W, Ikeda 8411
15. Chiadli A, Paic G (1982) Cross-section of (n,2n) reaction on ^{93}Nb and ^{90}Zr. Annual report of Univ. Mohammed, Rabat, Morocco 5:13
16. Bhika M, Saxena A, Roy BJ, Choudhury RK, Kailas S, Ganesan S (2017) Measurement of 67Zn(n, p)67Cu, 92Mo(n, p)92mNb and 98Mo(n, γ)99Mo reaction cross sections at incident neutron energies of En = 1.6 and 3.7 MeV. Nucl Sci Eng 163:175–182
17. Semkova V, Nolte R (2014) Measurement of neutron activation cross sections on Mo isotopes in the energy range from 7 MeV to 15 MeV. EPJ Web 66:03077
18. Wenrong Z, Hanlin L, Weixiang Y, Xiaogang H, Xiaolong H (1998) Measurement of cross section for ^{92}Mo(n,p)^{92m}Nb reaction and deduction of low energy neutron. INDC(CPR)-047/L
19. Molla NI, Miah RU, Sasunia S, Houssain SM, Rahman M (1997) Excitation functions of (n, p), (n, α) and (n,2n) processes on some isotopes of Cl, Cr, Ge, Mo and Ce in the energy range 13.57–14.71 MeV. TRIEST C 97 1:517
20. Kong X, Wang Y, Yuan J, Yang J (1996) The cross section measurements for the ^{92}Mo(n,p)^{92m}Nb, ^{98}Mo(n,p)^{98m}Nb and ^{94}Mo(n,2n)^{93m}Mo reactions. J Lanzhou Univ. ISSN: 0455-2059
21. Osman KT, Habbani FI (1996) Measurement and study of (n,p) reaction cross sections for Cr, Ti, Ni, Co, Zr and Mo isotopes using 14.7 MeV neutrons. INDC(SUD)-001
22. Kimura I, Kobayashi K (1990) Calibration fission and fusion neutron fields at the Kyoto University reactor. Nucl Sci Eng 106:332–344
23. Marcinkowski A, Stankiewicz K, Gauska U, Herman M (1986) Cross sections of fast neutron induced reactions on Molybdenum isotopes. Z Phys A Atomic Nuclei 323:91–96
24. Fessler A, Plompen AJM, Smith DL, Meadows JW, Ikeda Y (2000) Neutron activation cross section measurements from 16 to 20 MeV for isotopes of F, Na, Ma, Al, Si, P, Cl, Ti, V, Mn, Fe, Nb, Sn and Ba. Nucl Sci Eng 134:171–200
25. Garlea I, Miron-Garlea C, Rosh HN, Fodor G, Raduch V (1992) Integral neutron cross sections measured around 14 MeV. J Revue Roumaine de Phys 37:19
26. Amemiya S, Ishibashi K, Katoh T (1982) Neutron activation cross section of Molybdenum isotopes at 14.8 MeV. J Nucl Sci Technol 19(10):781–788
27. Quim SM, Woelfle R, Stoecklin G (1971) Activation cross sections of fast neutron induced nuclear reactions: precision measurements and systematics. Chemical Nuclear Data, Canterbury
28. Zolotarev KI (2010) Evaluation of cross-section data from threshold to 40 MeV for some neutron reactions important for fusion dosimetry applications. INDC (NDS)-0584
29. Zolotarev KI, Zolotarev PK (2013) Evaluation of some (n,n'), (n,γ), (n,p), (n,2n) and (n,3n) reaction excitation functions for fission and fusion reactor dosimetry applications. INDC (NDS)-0657
30. Csikai J (1982) Study of excitation function around 14 MeV neutron energy. In: Proceedings of the International Conference Antwerp, J Nucl Sci Technol, pp 414–417. https://doi.org/10.1007/978-94-009-7099-1
31. Filatenkov AA, Chuvaev SV, Aksenov VN, Jakovlev VA (1997) Systematic measurement of activation cross sections at neutron energies from 13.4 to 14.9 MeV. INDC (CCP)-402
32. Filatenkov AA (2016) Neutron activation cross sections measured at KRI in neutron energy region 13.4-14.9 MeV. INDC (CCP)-0406
33. IAEA-EXFOR Database available at http://www-nds.iaea.org/exfor
34. Koning AJ, Hilaire S, Goriely S (2015) TALYS-1.8, A Nuclear Reaction Program (NRG-1755 ZG Petten, The Netherlands). http://www.talys.eu/download-talys/
35. Sinha A, Roy T, Yogesh K, Ray N, Shukla M, Patel T, Bajpai S, Sarkar PS, Bishnoi S (2015) Experimental subcritical facility driven by D-D/D-T neutron generator at BARC, India. Nucl Instrum Methods Phys Res B 350:66–70
36. Kicka L (2016) Characterization of neutron fields around an intense neutron generator. Thesis. https://ir.library.dc-uoit.ca/handle/10155/758
37. NuDat 2.7 (2016) National Nuclear Data Center, Brookhaven National Laboratory. http://www.nndc.bnl.gov/nudat2
38. Martin MJ (2013) Nuclear data sheets for A = 152*. Nucl Data Sheets 114:1497–1847
39. Vidmar T (2005) EFFTRAN-A Monto Carlo efficiency transfer code for gamma-ray spectrometry. Nucl Instrum Methods Phys Res A 550:603–608
40. Geraldo LP, Smith DL (1990) Covariance analysis and fitting of germanium gamma-ray detector efficiency calibration data. Nucl Instrum Methods Phys Res A 290:499–508
41. Pasha I, Rudraswamy B, Radha E, Sathiamoorthy V (2018) Efficiency of high-purity germanium detector at characteristic gamma energies of ^{198}Au and ^{58}Co and covariance analysis. Radiat Prot Environ 41:110–114

42. Geraldo LP, Smith DL (1989) least square methods and covariance matrix applied to the relative efficiency calibration of a Ge(Li) detector. Inst de Pesquisas Energeticas e Nuleares 243:1–16
43. Millsap DW, Landsberger S (2015) Self-attenuation as a function of gamma ray energy in naturally occurring radioactive material in the oil and gas industry. Appl Radiat Isotopes 97:21–433
44. Nowotny R (1998) XMuDat: photon attenuation data on PC. IAEA Report IAEA-NDS 195. http://www-nds.iaea.org/publications/iaea-nds
45. Zsolnay EM, Capote Noy R, Nolthenius HJ, Trkov A (2014) International Reactor Dosimetry and Fusion File (IRDF 1.05). http://www-nds.iaea.org/IRDFF/
46. Yerraguntla SS, Naik H, Karantha MP, Ganesan S, Suryanarayana SV, Badwar S (2017) Measurement of 59Co(n, γ)60Co reaction cross sections at the effective neutron energies of 11.98 and 15.75 MeV. J Radioanal Nucl Chem 314(1):457–465
47. Santhi Sheela Y, Naik H, Prasad KM, Ganesan S, Suryanarayana S V (2017) Detailed data sets related to covariance analysis of the measurement of cross section of $^{59}Co(n,\gamma)^{60}Co$ reaction relative to the cross section of $^{115}In(n,\gamma)^{116m}In$. Internal Report, No. MU/STASTICS/DAE–BRNS/2017/3, 31 May 2017. https://doi.org/10.13140/rg.2.2.26729.49764
48. An International collaboration of NEA data bank participating countries (2017) The Joint Evaluated Fission and Fusion File (JEFF). http://www.oecd-nea.org
49. Zabrodskaya SV, Ignatyuk AV, Koscheev VN (2007) VANT, Nuclear constants. ROSFOND-2010, pp 1–2
50. Zsolnay EM, Capote R, Nolthenius HK, Trkov A (2012) Technical report. INDC(NDS)-0616, IAEA, Vienna
51. Shibata K, Iwamoto N, Kunieda S, Minato F, Iwamoto O (2016) Activation cross-section file for decommissioning of LWRs. JAEA, pp 47–52
52. Sublet J-Ch, Packer LW, Kopecky J, Forrest RA, Koning AJ, Rochman DA (2010) The European activation file: EAF-2010 neutron-induced cross section. CCFE-R 10:05
53. Blokhin AI, Gai EV, Ignatyuk AV, Koba II, Manokin VN (2016) New version of neutron evaluation data library BROND-3.1. Problems of atomic science and technology. Ser Nucl Reactor Constants 2:2–5
54. Sublet J-Ch, Koning AJ, Forrest RA, Kopecky J (2004) The JEFF-3.1/A. In: Proceedings of the conference on nuclear data for science and technology